Modern Physics Letters B, Vol. 7, No. 9 (1993) 573–590

THE VAN DER WAALS INTERACTION BETWEEN ALKALI MICROCLUSTERS

J. M. PACHECO
Departamento de Fisica da Universidade, 3000 Coimbra, Portugal

and

W. EKARDT
Fritz-Haber Institut der Max-Planck Gesellschaft, Faradayweg 4-6, 1000 Berlin 33, Germany

Received 3 March 1993

The nonretarded van der Waals coefficients C_6 and C_8 are determined for all pairs of neutral sodium and potassium microclusters with 1, 2, 8 and 20 atoms. The spherical jellium approximation is used to replace their ionic cores, and the valence electrons are treated in the local density approximation of density functional theory. The dynamical polarizabilities of these systems are computed making use of three different methods, two microscopic and quantum mechanical linear response formulations and one classical. It is found that quantum size effects, in particular Landau fragmentation, play a crucial role in the determination of these coefficients. Furthermore, we find that self-interaction errors present in standard microscopic approximations lead to sizeable effects in the strength of the van der Waals coefficients. On the other hand, we find that the vibrational temperature of these clusters has a very small effect in the van der Waals interaction which can be disregarded within the range of temperatures presently reachable experimentally.

1. Introduction

The van der Waals (dispersion) forces are present in the interaction between all kinds of atoms, molecules and surfaces. They play a very important role in many diverse areas of pure and applied science such as adhesion, surface tension, physical adsorption, flocculation or aggregation of particles in aqueous solutions, the structure condensed macromolecules such as proteins and polymers, etc. (see, e.g. Refs. 1, 2 and general references therein). Being typically relevant at large interatomic or intermolecular separations ($\approx$ 10 nm), still may play an important role down to distances of the order of few atomic radii (where many-body effects due to overlap of atomic densities begin to dominate the features of interatomic and intermolecular interactions) determining, in some cases, relative intermolecular orientation or inducing molecular rotational transitions.[3]

PACS Nos.: 36.40.+d, 31.50.+w, 33.20.Kf.

With the recent synthesis of new, gas-borne, ultra-fine particles[4,5] and of new forms of bulk matter,[6,7] the van der Waals interaction is expected to become of extreme importance in the description of cluster-cluster collisions[8–11] and associated growth of atomic and molecular clusters,[12] as well as in the characterization of relative orientation of clusters in bulk matter.[13,14] In what concerns these issues, most of the theoretical work devoted to the study of the van der Waals interaction between small metallic particles has been carried out using classical electrodynamics to describe their dynamic polarizabilities (cf., however, Ref. 15). It is by now established, however, that Quantum Size Effects (QSE) play a crucial role in many properties of these small metallic particles (also in what concerns their dynamical polarizability) a feature which, being absent in the classical treatment requires, *per se*, a quantum mechanical formulation.

In this paper, we shall compute the leading order coefficients C_6 and C_8 of the van der Waals interaction between pairs of neutral microclusters of alkali atoms. These coefficients, as we shall discuss in the next section, constitute essential ingredients necessary to fully characterize the above mentioned interaction. We shall consider sodium and potassium, and compute the interaction coefficients between all pairs of sodium and potassium "magic" clusters with 1, 2, 8 and 20 constituent atoms. We make use of the Spherical Jellium Uniform Background Model (SJUBM) and of Density Functional Theory (DFT) in the Local Density Approximation (LDA)[16] for the description of the Ground State (GS) properties of sodium and potassium clusters, and linear response theory for the calculation of the dynamic polarizabilities. We shall consider two different levels of calculation of the properties of these microclusters: The standard LDA calculation, and the associated Time Dependent LDA (TDLDA) linear response formulation,[17,18] and also we shall compute the dynamic polarizabilities implementing the Self-Interaction Corrections (SIC) both at the level of the ground state in the way proposed by Perdew and Zunger[19] called SIC-LDA and at the level of linear response in the formulation developed recently by the authors[20] entitled FULL-SIC-TDLDA. This is due to the fact that it has been shown recently[20,21] that the self-interaction errors present in the standard LDA and TDLDA formulations lead to sizeable consequences in the computation of the static and dynamic polarizabilities of alkali microclusters (this result applies, generally, to all finite many-electron systems). Both formulations are fully self-consistent. This is by now recognized as a necessary feature of any microscopic calculation aiming at producing reliable QSE.[22] These, in turn, will be shown to play a crucial role also in the determination of the van der Waals coefficients. Furthermore, the classical plasmon-pole approximation, which leads to analytical expressions for the van der Waals coefficients, will be also considered in the present paper. A preliminary account of some of these results has been published elsewhere.[23]

This paper is organized as follows: In Sec. 2 the formalism is presented and the microscopic formulations we use reviewed. Furthermore, the (analytic) results of the classical plasmon-pole approximation will be reviewed as well. Section 3 is

devoted to the presentation and discussion of the results obtained and their expected accuracy, as well as to the discussion of the influence of other effects such as the vibrational temperature of the intervening clusters. Section 4 contains the main conclusions and future prospects.

2. Formalism

The nonretarded electrostatic interaction energy between two clusters A and B, at a distance R large enough so that their charge densities do not overlap, can be written in the form,[2]

$$\Delta E = -\frac{C_6^{AB}}{R^6} - \frac{C_8^{AB}}{R^8} - \cdots \ . \tag{1}$$

In this way one formally singles out the distance dependence of the interaction energy, in the traditional power expansion. In general however, the coefficients C_k^{AB} carry information on the species A and B involved, the detailed features of their electronic response and on the relative orientation of the two clusters. This is because they can be generally expressed in terms of the polarizabilities of the intervening clusters which, being second rank tensors, lead eventually to rather lengthy expressions. This situation is greatly simplified when the intervening clusters are spherical. This will be the case for all clusters considered in this paper, to which the spherical approximation has proven very successful. For spherically symmetric objects, angular momentum is a good quantum number and a multipole decomposition of the dynamic polarizabilities is appropriate. In such conditions, the van der Waals coefficients can be expressed,[24,25] making use of the dynamic multipole polarizabilities $\alpha_L(\omega)$, by

$$C_6^{AB} = C(A,1;B,1) \ , \quad C_8^{AB} = C(A,1;B,2) + C(A,2;B,1) \tag{2}$$

with

$$C(A,L_1;B,L_2) = \frac{(2L_1+2L_2)!}{\pi^2(2L_1)!(2L_2)!}\int_0^{+\infty} d\omega_1 \ \mathrm{Im}[\alpha_{L_1}^A(\omega_1)] \times \int_0^{+\infty} \frac{d\omega_2}{\omega_1+\omega_2}\mathrm{Im}[\alpha_{L_2}^B(\omega_2)] \ , \tag{3}$$

In the above equation, $\mathrm{Im}[\alpha_L^K(\omega)]$ stands for the imaginary part of the dynamic polarizability α of cluster $K(K = A,B)$ and multipolarity L, evaluated at the real frequency ω. It is then clear that C_6^{AB} results from the dipole-dipole interaction between clusters A and B, C_8^{AB} results from the dipole-quadrupole interaction between these two clusters, etc. Since the determination of the van der Waals coefficients requires the calculation of the dynamic multipole polarizabilities of the different clusters, which are proportional to the electronic response of the cluster to an external perturbation of multipolarity L, the properties of these coefficients will depend crucially on the detailed features of the electronic response. It is

worth mentioning that the above expression, Eq. (3), is written in a non-standard fahion. Indeed, it is common practice to write down the interaction coefficients $C(A, L_1; B, L_2)$ in terms of the polarizability computed at an imaginary frequency iu, which is a real function of u. In terms of these quantities, Eq. (3) reads, then,

$$C(A, L_1; B, L_2) = \frac{(2L_1 + 2L_2)!}{2\pi(2L_1)!(2L_2)!} \int_0^{+\infty} du \alpha^A_{L_1}(iu)\alpha^B_{L_2}(iu) \ . \tag{4}$$

These are two equivalent ways of calculating the same quantity and are obtained by direct substitution of the definition of the polarizability in the standard result of second order perturbation theory (for a general proof, cf. Ref. 24). However, since $\mathrm{Im}[\alpha^K_L(\omega)]$ is directly related to the photoabsorption cross-section (which can be measured experimentally), we shall perform our calculations making use of Eq. (3).

In the remaining part of this section, we shall critically review the microscopic determination of the dipole ($L = 1$) and quadrupole ($L = 2$) dynamic polarizabilities of neutral sodium and potassium clusters with 1, 2, 8 and 20 atoms.

Within the jellium model, the rigid (positively charged) background, which crudely replaces the ionic structure of the microclusters, is unpolarizable, providing solely an external potential under the influence of which the valence electrons of each constituent atom of the microcluster move. Therefore, all contributions to the polarizability of the cluster arises from their electronic degrees of freedom.

The LDA description of alkali microclusters within the jellium model has been extremely successful in providing a simple yet accurate (to within 15%) understanding of many GS and response properties of sp-bonded metal clusters. It was making use of the jellium model plus LDA that the shell structure of these small aggregates of alkali atoms has been theoretically predicted.[16] Furthermore, the jellium model constitutes, at present, the only workable framework which can provide results for clusters over a wide range of atomic constituents, providing unique information on a novel field of physics which is able to bridge the gap between a single atom and a piece of bulk metal. However, with the recent availability of new experimental information, the flaws of the jellium model and LDA have become more prominent, and improvements of the LDA have been sought. This is because the comparison of LDA calculations incorporating the ionic degrees of freedom with corresponding calculations making use of the jellium approximation show that the jellium model works very well.[26] Of the different improvements of the LDA which have been developed, and to our knowledge the only one which preserves the essential features of self-consistency and linearity which constitute the benchmark of the success of LDA and TDLDA, has been the FULL-SIC-TDLDA.[20] Furthermore this formulation, when applied to the computation of response properties of metal microclusters, provides the best overall agreement obtained so-far between the theoretical and experimental photoabsorption features of both neutral and charged alkali microclusters.[20] On the foregoing, we shall review briefly the underlying features pertaining to all of these formulations, as well as to the classical plasmon-pole

approximation which, though lacking any QSE, leads to simple analytic results for the van der Waals coefficients.

To describe the GS of a cluster with $\aleph$ ions and N valence electrons, in the LDA, we start by solving the Kohn–Sham equations,

$$\left[\frac{-\hbar^2}{2m}\Delta + V_{\rm MF}(\mathbf{r})\right]\psi_j(\mathbf{r}) = \varepsilon_j\psi_j(\mathbf{r}) \ , \tag{5}$$

where the LDA mean-field (MF) potential reads,

$$V_{\rm MF}(\mathbf{r}) = V_I(\mathbf{r}) + e^2\int\frac{n(\mathbf{r}_1)d\mathbf{r}_1}{|\mathbf{r}-\mathbf{r}_1|} + V_{\rm xc}[n(\mathbf{r})] \ , \quad n(\mathbf{r}) = \sum_{j=1}^{N}|\psi_j(\mathbf{r})|^2 \ . \tag{6}$$

$V_I(\mathbf{r})$ is the jellium potential of $\aleph$ positive ions; $\psi_j(\mathbf{r})$ represents the eigenfunction with quantum number j, and ε_j is the corresponding eigenvalue. $V_{\rm xc}$ is the LDA for Exchange and Correlation (XC) for which we use the parametrization of Gunnarsson and Lundqvist.[27] As is clear from the above definition of the average potential, each electron interacts with itself spuriously via the construction of the total electronic potential by means of the *total* density. The SIC attempts at correcting for this deficiency in the average potential, by replacing the above scheme by a similar one, in which a set of Kohn–Sham-like equations is still solved, but now with an orbital dependent potential:

$$\left[\frac{-\hbar^2}{2m}\Delta + \tilde{V}^{(i)}_{\rm SIC}(\mathbf{r})\right]\tilde{\psi}^{(i)}_j(\mathbf{r}) = \tilde{\varepsilon}^{(i)}_j\tilde{\psi}^{(i)}_j(\mathbf{r}) \ , \tag{7}$$

where $\tilde{V}^{(i)}_{\rm SIC}$ is related to $V_{\rm MF}$ by,

$$\tilde{V}^{(i)}_{\rm SIC}(\mathbf{r}) = V_{\rm MF}(\mathbf{r}) - e^2\int\frac{\tilde{n}_i(\mathbf{r}_1)d\mathbf{r}_1}{|\mathbf{r}-\mathbf{r}_1|} - V_{\rm xc}[\tilde{n}_i(\mathbf{r})] \ , \quad \tilde{n}_i(\mathbf{r}) = |\tilde{\psi}^{(i)}_i(\mathbf{r})|^2 \ . \tag{8}$$

To make the notation unambiguous, we redefined the eigenfunctions and eigenvalues, such that $\tilde{\psi}^{(i)}_j(\mathbf{r})$ represents the eigenfunction of orbital potential $\tilde{V}^{(i)}_{\rm SIC}$ with quantum numbers j, and $\tilde{\varepsilon}^{(i)}_j$ the corresponding eigenvalue. Furthermore, we shall consistently denote by X a given self-interacting quantity and by $\tilde{X}$ the corresponding quantity in the SIC case. In this notation the total density appearing in $V_{\rm MF}$ is now defined as[28]

$$\tilde{n}(\mathbf{r}) = \sum_{i=1}^{N}|\tilde{\psi}^{(i)}_i(\mathbf{r})|^2 \ . \tag{9}$$

We would like to point out that, contrary to the self-interacting case, in which the Kohn-Sham eigenvalues and eigenfunctions have no direct relation to the quasiparticle energies and wave functions of the cluster, the SIC-LDA solutions constitute good candidates for the representation of these quantities.[19]

We shall consider now the general theory of linear response to an external perturbation, starting with the self-interacting case (TDLDA) and including the SIC later.

Under the action of an external, time-dependent perturbation of the form

$$V_{\rm ext}(\mathbf{r}) = -r^L P_L(\cos\theta)\cos(wt) \ , \tag{10}$$

the valence electrons will respond, to zero order, independently. The independent particle induced density will oscillate in phase with the external perturbation, its single Fourier component being given by

$$\delta n_0(\mathbf{r},\omega) = \int d\mathbf{r}_1 \chi_0(\mathbf{r},\mathbf{r}_1;\omega) V_{\rm ext}(\mathbf{r}_1,\omega) \ , \tag{11}$$

where the independent particle susceptibility can be written in the form,

$$\chi_0(\mathbf{r},\mathbf{r}_1;\omega) = \sum_i^{\rm occ} \psi_i^*(\mathbf{r})\psi_i(\mathbf{r}_1) G(\mathbf{r},\mathbf{r}_1,\varepsilon_i+\hbar\omega) + \psi_i(\mathbf{r})\psi_i^*(\mathbf{r}_1) G^*(\mathbf{r},\mathbf{r}_1,\varepsilon_i-\hbar\omega) \ . \tag{12}$$

In the above equation, G is the retarded Green's function associated with the LDA Schrödinger-type equation,

$$\left[E + \frac{\hbar^2}{2m}\Delta - V_{\rm MF}(\mathbf{r})\right] G(\mathbf{r},\mathbf{r}_1,E) = \delta(\mathbf{r}-\mathbf{r}_1) \ . \tag{13}$$

Note that each Green's function includes all possible single-electron excitations from a specific orbital, including transitions which are forbidden by the Pauli principle. These, however, are exactly cancelled by the combination of Green's functions in Eq. (12) (for details, cf. Ref. 20).

As is well known, the independent particle approximation overestimates the response of the system to an external perturbation. This is because the screening of the external perturbation due to the induced density is not taken into account. In linear response, one includes this field by requiring a self-consistency condition between the induced density and the screening potential. Denoting the linearly induced density by δn and expanding the potential in Eq. (6) keeping only the linear terms we get,

$$V_{\rm screen}(\mathbf{r},\omega) = e^2 \int \frac{\delta n(\mathbf{r}_1,\omega) d\mathbf{r}_1}{|\mathbf{r}-\mathbf{r}_1|} + \frac{\delta V_{\rm xc}[n(\mathbf{r})]}{\delta n} \delta n(\mathbf{r},\omega) \ . \tag{14}$$

The linear response equation for δn reads, then,

$$\delta n(\mathbf{r},\omega) = \int d\mathbf{r}_1 \chi_0(\mathbf{r},\mathbf{r}_1;\omega)[V_{\rm ext}(\mathbf{r}_1,\omega) + V_{\rm screen}(\mathbf{r}_1,\omega)] \ . \tag{15}$$

This equation, together with the definition of $V_{\rm screen}$, Eq. (14), constitute the TDLDA equations for the induced density. We proceed now by correcting this formulation including SIC.

Since, in SIC-LDA, the single-particle potentials are orbital dependent, the independent particle susceptibility is conveniently rewritten as

$$\begin{aligned}\widetilde{\chi_0}(\mathbf{r},\mathbf{r}_1;\omega) &= \sum_i^{\text{occ}} \tilde{\psi}_i^{(i)*}(\mathbf{r})\tilde{\psi}_i^{(i)}(\mathbf{r}_1)\tilde{G}^{(i)}(\mathbf{r},\mathbf{r}_1,\tilde{\varepsilon}_i^{(i)}+\hbar\omega) \\ &\quad + \sum_i^{\text{occ}} \tilde{\psi}_i^{(i)}(\mathbf{r})\tilde{\psi}_i^{(i)*}(\mathbf{r}_1)\tilde{G}^{(i)*}(\mathbf{r},\mathbf{r}_1,\tilde{\varepsilon}_i^{(i)}-\hbar\omega) \\ &= \sum_i^{\text{occ}} \tilde{\Lambda}^{(i)}(\mathbf{r},\mathbf{r}_1,\omega)\ . \end{aligned} \tag{16}$$

The (orbital dependent) Green's functions $\tilde{G}^{(i)}$ are now related to the solution of the following equation

$$\left[E+\frac{\hbar^2}{2m}\Delta-\tilde{V}_{\text{SIC}}^{(i)}(\mathbf{r})\right]\hat{G}^{(i)}(\mathbf{r},\mathbf{r}_1,E)=\delta(\mathbf{r}-\mathbf{r}_1) \tag{17}$$

by

$$\tilde{G}^{(i)}(\mathbf{r},\mathbf{r}_1,\tilde{\varepsilon}_i^{(i)}+\hbar\omega)=\left[\widehat{G}^{(i)}(\mathbf{r},\mathbf{r}_1,\tilde{\varepsilon}_i^{(i)}+\hbar\omega)-\sum_j^{\text{occ}}\frac{\tilde{\psi}_j^{(i)}(\mathbf{r})\tilde{\psi}_j^{(i)*}(\mathbf{r}_1)}{\tilde{\varepsilon}_i^{(i)}+\hbar\omega-\tilde{\varepsilon}_j^{(i)}+i\delta}\right]\ . \tag{18}$$

The physics associated with the above equations is quite simple. Because the potential is orbital dependent, the transitions from a given occupied state should be computed with the potential appropriate for this state. $\tilde{G}^{(i)}$ is obtained from $\widehat{G}^{(i)}$ through Eq. (18). The additional terms explicitly avoid any violation of the Pauli principle, since in the SIC case, the Pauli-forbidden upward transitions originate from a different potential than the corresponding Pauli-forbidden downward transitions.[20]

We proceed now to correct for the self-interaction errors in the screening potential. From the definition of V_{screen} in Eq. (14) it is clear that there is a spurious self-interaction due to the fact that this potential is calculated with the total induced density. The appropriate screening term to incorporate in a self-interaction free theory is an orbital dependent screening which reads (cf. Eq. (14) and Ref. 20),

$$\tilde{V}_{\text{screen}}^{(i)}(\mathbf{r},\omega)=e^2\int\frac{[\delta\tilde{n}(\mathbf{r}_1,\omega)-\delta\tilde{n}^{(i)}(\mathbf{r}_1,\omega)]d\mathbf{r}_1}{|\mathbf{r}-\mathbf{r}_1|}+\frac{\delta V_{\text{xc}}[\tilde{n}(\mathbf{r})]}{\delta n}[\delta\tilde{n}(\mathbf{r},\omega)-\delta\tilde{n}^{(i)}(\mathbf{r},\omega)]\ , \tag{19}$$

where $\delta\tilde{n}^{(i)}(\mathbf{r})$ are now the orbital contributions to the total SIC screened induced density

$$\delta\tilde{n}(\mathbf{r},\omega)=\sum_i^{\text{occ}}\delta\tilde{n}^{(i)}(\mathbf{r},\omega)\ . \tag{20}$$

Equation (20) together with Eqs. (16) and (19) enable us to write now a system of coupled equations (as many as the number of occupied orbitals) constituting the FULL-SIC-TDLDA equations:

$$\delta\tilde{n}^{(i)}(\mathbf{r},\omega) = \int d\mathbf{r}_1 \tilde{\Lambda}^{(i)}(\mathbf{r},\mathbf{r}_1,\omega)[V_{\rm ext}(\mathbf{r}_1,\omega) + \tilde{V}^{(i)}_{\rm screen}(\mathbf{r}_1,\omega)] \ . \tag{21}$$

The general solution for $\delta\tilde{n}$ is non-trivial, even at the TDLDA level, and has in this case been carried out only for a restricted class of geometries of the jellium backgrounds.[18,29] When the number of valence electrons corresponds to a "magic number" (as is the case for all clusters considered in this work) a spherical shape of the jellium background gives the appropriate choice, the N electrons filling completely a given number of spherical electronic shells. Angular momentum is therefore a good quantum number, and the problem is best solved in spherical coordinates. Moreover, the response to an external field of well defined multipolarity is diagonal in L and the polarizability of multipolarity L is related to the L-component $\delta\tilde{n}_L(r,\omega)$, being written as,

$$\alpha_L(\omega) = -e^2 \frac{4\pi}{2L+1} \int_0^{+\infty} dr \ r^{L+2} \delta\tilde{n}_L(r,\omega) \ . \tag{22}$$

Finally, we would like to introduce the classical plasmon-pole approximation, and its analytic results for the dynamic polarizability. In this approximation all the strength of the multipole response is concentrated in a single peak, and we may write[15] ($K = A, B$),

$$\mathrm{Im}[\alpha^K_L(\omega)] = \frac{\pi}{2}\omega^K_L R^{2L+1}_K \delta(\omega - \omega^K_L) \ , \tag{23}$$

with

$$\omega^K_L = d_L \omega^K_p = \sqrt{\frac{L}{2L+1}}\omega^K_p \ , \tag{24}$$

and

$$R_K = r_{s,K} \aleph^{\frac{1}{3}} \ , \tag{25}$$

where $r_{s,K}$ the Wigner-Seitz radius of cluster species K in atomic units (4 for sodium and 4.86 for potassium) and $\aleph$ the number of ions in the cluster. ω^K_p is the plasma frequency in the bulk and is given by,

$$\hbar\omega^K_p = [47.1 \ eV] r^{-3/2}_{s,K} \ . \tag{26}$$

With the above representation for the polarizability, the van der Waals coefficients can be obtained by analytic integration of Eq. (3) leading to the following expressions for the general interaction between clusters of arbitrary species A and B:

$$C_6 = \frac{3}{2}(R_A R_B)^3 d_1 \frac{\omega^A_p \omega^B_p}{\omega^A_p + \omega^B_p} \ ,$$

$$C_8 = \frac{15}{4}(R_A R_B)^3 \omega^A_p \omega^B_p d_1 d_2 \left[\frac{R^2_B}{d_1\omega^A_p + d_2\omega^B_p} + \frac{R^2_A}{d_2\omega^A_p + d_1\omega^B_p} \right] .$$

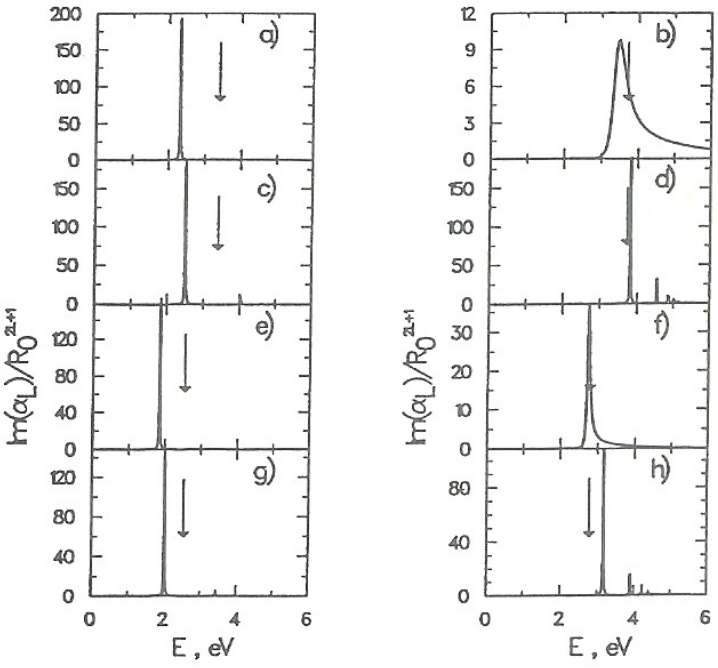

Fig. 1. Imaginary part of the dynamic polarizabilities of sodium and potassium atoms. Left column contains results for the dipole polarizabilities ($L = 1$) whereas the right column contains the quadrupole polarizabilities ($L = 2$). Parts a), b), c), and d) contain results for sodium, the remaining 4 curves corresponding to potassium. Parts a), b), e), and f) display results obtained making use of the TDLDA, whereas the remaining parts contain results using the FULL-SIC-TDLDA. The polarizabilities are plotted in dimensionless units since, for each part, they have been divided by $R_K^{(2L+1)}$, where L is the multipolarity and R_K is given by Eq. (25). In each part, the vertical arrow indicates the (size independent, cf. Eq. (24)) position of the single plasmon peak in the plasmon-pole approximation.

3. Results and Discussion

We determined the dipole ($L = 1$) and quadrupole ($L = 2$) dynamic polarizabilities of neutral sodium and potassium clusters, with 1, 2, 8, and 20 constituent atoms. We used the SJUBM with the LDA and SIC-LDA for the description of the GS properties of the clusters, the determination of the screened electronic multipole response[30] being computed in both TDLDA and FULL-SIC-TDLDA. The corresponding results are shown in Figs. 1 to 4. Each figure concerns one specific number of atomic constituents, namely: Fig. 1 shows results for the atom, Fig. 2 for the dimer, etc. in ascending order of atomic constituents. Each of the figures contains eight parts, arranged in four lines and two columns. Each left column contains the dipole response whereas each right column contains the quadrupole response. The first two lines of each figure display the results for sodium, whereas the last two lines display the results for potassium. Finally, parts a), b), e) and f), show the TDLDA results, whereas parts c), d), g) and h) show the FULL-SIC-TDLDA results. In all figures, vertical arrows indicate the (size independent) peak

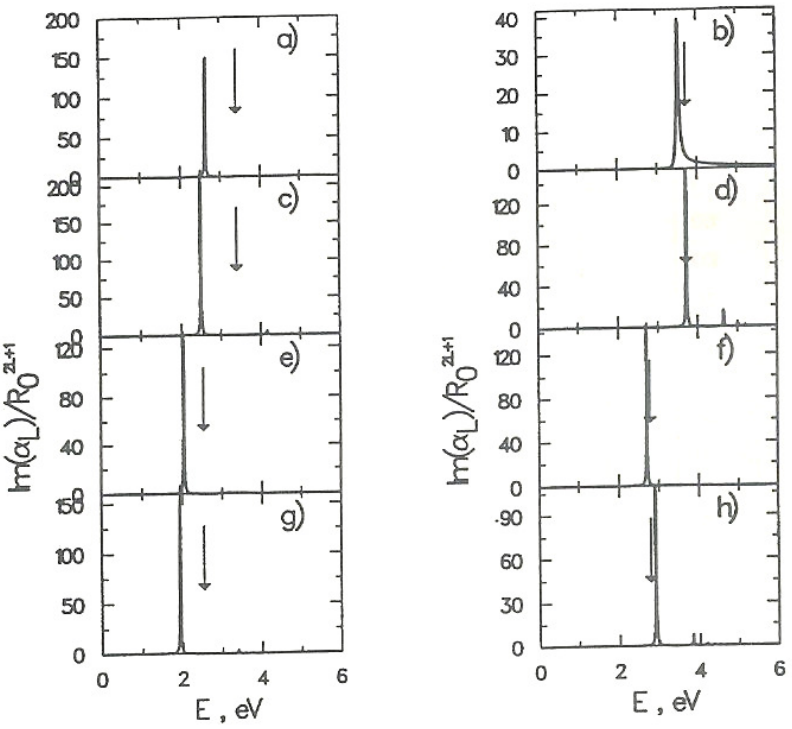

Fig. 2. Imaginary part of the dynamic polarizabilities of sodium and potassium clusters with 2 constituent atoms (same conventions and notation as in Fig. 1).

position of the dynamic multipole polarizabilities calculated in the plasmon-pole approximation. As becomes clear from Figs. 1 to 4, there are large differences between the results of the microscopic calculations and the classical approximation, which will reflect upon the calculated values for the C_6 and C_8 coefficients. Indeed, the microscopic responses evidence an overall redshift with respect to their classical counterpart, and also a sizeable amount of Landau fragmentation, leading to the multi-peaked structures displayed in the figures. Both QSE have been detected experimentally (for $L = 1$) by measuring the photoabsorption cross section of these small metallic systems,[31] which clearly indicates that the plasmon-pole approximation is inadequate for describing the response of small clusters.

As compared to the TDLDA, the FULL-SIC-TDLDA dipole polarizabilities show a further red-shift of the main plasmon peak (except for the atoms and the $L = 2$ mode of the dimers), a feature which correlates systematically with the available experimental evidence. Furthermore, it predicts the occurrence of extra structure in the ultra-violet part of the spectrum, which still waits for an unambiguous experimental confirmation. This feature, however, correlates well with the well-known problem of the missing strength in the experimental data.[31] In this way, one can expect further differences between the van der Waals coefficients obtained making use of the TDLDA and the FULL-SIC-TDLDA dynamic polarizabilities. In keeping with this discussion one expects, therefore, the FULL-SIC-TDLDA results to be the most accurate of all results presented in this paper.

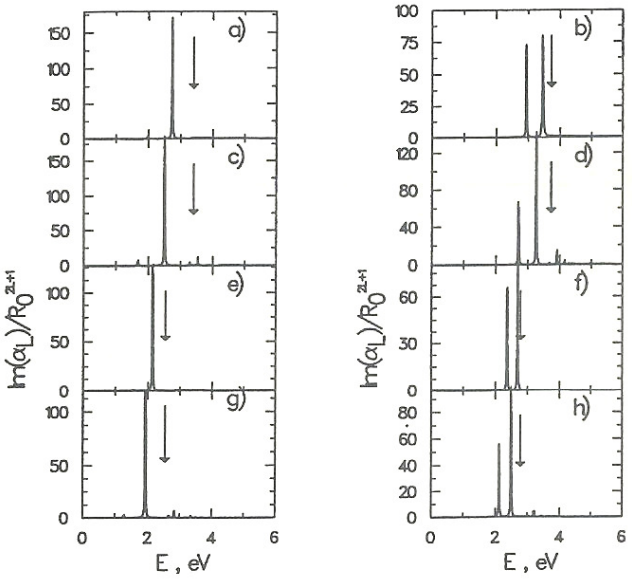

Fig. 3. Imaginary part of the dynamic polarizabilities of sodium and potassium clusters with 8 constituent atoms (same conventions and notation as in Fig. 1).

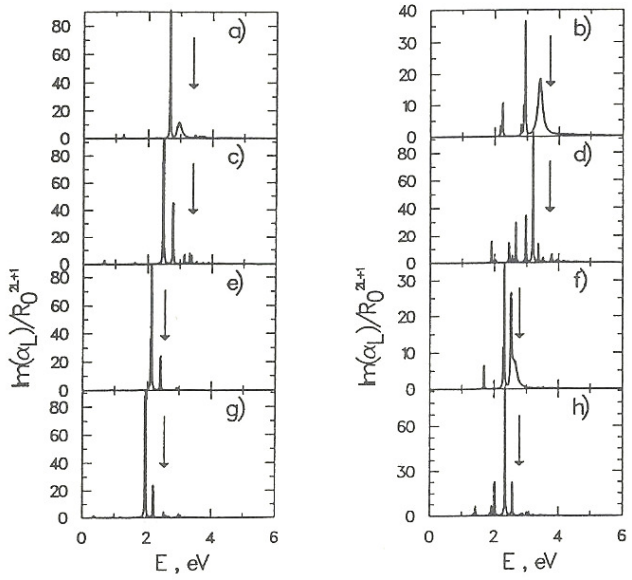

Fig. 4. Imaginary part of the dynamic polarizabilities of sodium and potassium clusters with 20 constituent atoms (same conventions and notation as in Fig. 1).

Table 1. Values for the van der Waals coefficient C_6 (in $eV\ a_0^6$) for the pair interaction between sodium clsuters with 1, 2, 8, and 20 constituent atoms. For each entry, the first line gives the values calculated making use of the FULL-SIC-TDLDA, the second line the values calculated via TDLDA and the third line the classical result obtained making use of the plasmon pole approximation (see main text). The numbers follow the notation: $2.49(4) = 2.49\ 10^4$.

N	1	2	8	20
	2.32(4)	4.75(4)	1.82(5)	4.23(5)
1	2.49(4)	4.21(4)	1.64(5)	3.93(5)
	1.04(4)	2.09(4)	8.35(4)	2.09(5)
		9.74(4)	3.73(5)	8.67(5)
2		7.12(4)	2.78(5)	6.66(5)
		4.18(4)	1.67(5)	4.18(5)
			1.43(6)	3.32(6)
8			1.09(6)	2.60(6)
			6.68(5)	1.67(6)
				7.73(6)
20				6.22(6)
				4.18(6)

Table 2. Values for the van der Waals coefficient C_8 (in $eV\ a_0^8$) for the pair interaction between sodium clusters with 1, 2, 8, and 20 constituent atoms (same conventions and notation as in Table 1).

N	1	2	8	20
	1.75(6)	4.09(6)	3.55(7)	1.51(8)
1	1.88(6)	3.97(6)	3.33(7)	1.38(8)
	8.73(5)	2.26(6)	1.75(7)	7.31(7)
		9.42(6)	7.67(7)	3.19(8)
2		8.08(6)	6.17(7)	2.47(8)
		5.55(6)	3.90(7)	1.56(8)
			4.50(8)	1.58(9)
8			3.59(8)	1.25(9)
			2.24(8)	7.94(8)
				4.93(9)
20				3.92(9)
				2.57(9)

Table 3. Values for the van der Waals coefficient C_6 (in $eV\ a_0^6$) for the pair interaction between potassium clusters with 1, 2, 8, and 20 constituent atoms (same conventions and notation as in Table 1).

N	1	2	8	20
	4.57(4)	9.96(4)	3.81(5)	8.93(5)
1	5.80(4)	9.96(4)	3.70(5)	8.62(5)
	2.51(4)	5.02(4)	2.01(5)	5.02(5)
		2.17(5)	8.30(5)	1.95(6)
2		1.71(5)	6.37(5)	1.49(6)
		1.00(5)	4.01(5)	1.00(6)
			3.18(6)	7.45(6)
8			2.37(6)	5.52(6)
			1.60(6)	4.01(6)
				1.75(7)
20				1.29(7)
				1.00(7)

Once the dynamic polarizabilities have been determined, the van der Waals coefficients are obtained by direct integration of Eq. (3). The results are given in Tables 1–6. Tables 1–4 consider the van der Waals coefficients for the interaction between clusters of the same species namely, sodium (Tables 1 and 2) and potassium (Tables 3 and 4) whereas Tables 5 and 6 contain the values relative to the interaction between a sodium and a potassium cluster. The values quoted are all in eVa_0^6 for the C_6 coefficient, and eVa_0^8 for the C_8 coefficient. Tables 1, 3 and 5 contain values for C_6 while Tables 2, 4 and 6 contain values for C_8. For each entry in any table, three numbers are given. The upper value corresponds to the one we expect to be most accurate, namely, the FULL-SIC-TDLDA value. In the middle, the TDLDA result is presented and in the bottom the classical result is tabulated. As is clear already from the figures, the classical description of the dynamic polarizabilities is, in most cases, quite unrealistic. Therefore, the discrepancies between the classical and the quantum mechanical results tabulated are of no surprise. On the other hand, the discrepancies between the values of the van der Waals coefficients obtained with the two quantum mechanical methods are due to the sizeable effect of the self-interaction errors present in the LDA, and, to a large extent, eliminated in the FULL-SIC-TDLDA. Since these errors are larger the smaller the system, the deviations are not systematic, and it is difficult to characterize them in general terms. For the larger clusters ($N > 2$), the coefficients obtained with FULL-SIC-TDLDA are systematically larger than their TDLDA counterparts. The reverse happens for the atoms, which is directly related to the different effect of SIC in these systems as compared to the larger clusters. Although this is supported by

other calculations (cf., e.g., Ref. 32), it is clear, however, that to treat the atom in the jellium approximation constitutes a very drastic oversimplication. In fact, the SJUBM is best suited for larger clusters, and in this sense the atomic results presented here correspond to a rather extreme extrapolation which was carried out since we are unaware of any experimental data and/or theoretical predictions for these systems, except for the atomic species. Indeed, the available experimental data has been combined with extensive atomic calculations in Ref. 33 to determine lower and upper bounds for the van der Waals coefficients. The results are reproduced in Table 7. These may be subject to revision (cf. e.g., Ref. 34), in the sense that they are very sensitive to the input data which is not complete and unambiguously established. Furthermore (as pointed out in Ref. 33), the authors of Ref. 33 believe the true values for the C_6 and C_8 coefficients to be closer to the lower bounds than to the upper bounds, which is supported by our results.

All results tabulated were obtained making use of theories which do not incorporate the finite linewidth associated with both dipole and quadrupole collective excitations. However, and to the extent that the intrinsic width of each peak is small compared to the distance between consecutive peaks, one can still expect the predictions of these theories to be reliable.

At the level of the dipole response, the finite linewidth of the different peaks in the photoabsorption cross-section has been successfully interpreted in terms of two processes[35–37]: 1. Fluctuations of the cluster surface; 2. Collisions with the ionic phonons.

Table 4. Values for the van der Waals coefficient C_8 (in $eV\ a_0^8$) for the pair interaction between potassium clusters with 1, 2, 8, and 20 constituent atoms (same conventions and notation as in Table 1).

N	1	2	8	20
	4.15(6)	1.10(7)	1.04(8)	4.55(8)
1	6.54(6)	1.43(7)	1.09(8)	4.52(8)
	3.10(6)	8.01(6)	6.19(7)	2.59(8)
		2.81(7)	2.44(8)	1.03(9)
2		2.98(7)	2.07(8)	8.25(8)
		1.97(7)	1.38(8)	5.55(8)
			1.45(9)	5.15(9)
8			1.13(9)	3.90(9)
			7.93(8)	2.82(9)
				1.62(10)
20				1.21(10)
				9.13(9)

Table 5. Values for the van der Waals coefficient C_6 (in $eV\ a_0^6$) for the pair interaction between sodium clusters (values for N along the column) and potassium clusters (values for N along the line) with 1, 2, 8, and 20 constituent atoms (same conventions and notation as in Table 1). Note that the classical approximation leads to the same value for the C_6 coefficient of the pair interactioins $[Na_X, K_Y]$ and $[Na_Y, K_X]$. The asymmetry of these pair interactions in the microscopic results is due to QSE.

N	1	2	8	20
	3.24(4)	7.03(4)	2.69(5)	6.32(5)
1	3.77(4)	6.51(4)	2.42(5)	5.66(5)
	1.60(4)	3.20(4)	1.28(5)	3.20(5)
	6.64(4)	1.44(5)	5.52(5)	1.29(6)
2	6.30(4)	1.09(5)	4.07(5)	9.50(5)
	3.20(4)	6.40(4)	2.56(5)	6.40(5)
	2.54(5)	5.52(5)	2.11(6)	4.96(6)
8	3.36(5)	5.87(5)	2.19(6)	5.12(6)
	1.28(5)	2.56(5)	1.02(6)	2.56(6)
	5.90(5)	1.28(6)	4.91(6)	1.15(7)
20	5.88(5)	1.02(6)	3.81(6)	8.88(6)
	3.20(5)	6.40(5)	2.56(6)	6.40(6)

Table 6. Values for the van der Waals coefficient C_8 (in $eV\ a_0^8$) for the pair interaction between sodium and potassium clusters with 1, 2, 8, and 20 constituent atoms (same conventions and notation as in Table 5).

N	1	2	8	20
	2.70(6)	7.24(6)	7.22(7)	3.18(8)
1	3.56(6)	8.14(6)	6.70(7)	2.87(8)
	1.66(6)	4.49(6)	3.72(7)	1.60(8)
	6.23(6)	1.64(7)	1.54(8)	6.66(8)
2	7.17(6)	1.57(7)	1.20(8)	5.01(8)
	4.10(6)	1.05(7)	8.06(7)	3.35(8)
	5.13(7)	1.22(8)	8.17(8)	3.09(9)
8	6.04(7)	1.23(8)	7.93(8)	3.05(9)
	2.92(7)	6.78(7)	4.25(8)	1.60(9)
	2.14(8)	4.90(8)	2.69(9)	9.02(9)
20	2.18(8)	4.10(8)	2.11(9)	6.98(9)
	1.18(8)	2.59(8)	1.42(9)	4.89(9)

Both mechanisms depend on the vibrational temperature of the clusters, but their dependence is different. Indeed, while the first process leads to a line width increasing with the square root of the temperature,[35,37,38] the second process is ex-

Table 7. Lower and Upper bounds (taken from Ref. 33) for the van der Waals coefficients C_6 and C_8 corresponding to the interaction between pairs of sodium and potassium atoms. Units and notation as in Tables 1–6.

	C_6		C_8	
	lower	*upper*	*lower*	*upper*
$Na-Na$	4.00(4)	1.36(5)	2.86(6)	5.47(6)
$Na-K$	5.56(4)	9.99(4)	5.52(6)	8.08(6)
$K-K$	1.08(5)	1.10(5)	1.04(7)	1.09(7)

pected to exhibit a linear dependence.[36,37] For the room-like temperatures achieved in present day experiments, the first mechanism provides the dominant contribution. However, and as the van der Waals coefficients are concerned, these processes provide an extra line width which can be simulated[35] by folding the electronic response with Gaussian functions with widths compatible with the magnitude of the relaxation mechanisms involved. Similar outcome is expected for the quadrupole response, even though the mechanisms may be different. On the other hand, and for this temperature range, the QSE obtained at the level of linear response, corresponding to the so-called Landau fragmentation, remain essentially unchanged, due to the fact that the energy gap between filled and empty shells is nearly temperature independent[39] and much larger than the vibrational temperature. We checked the reliability of our predictions by recalculating the C_6 coefficients, within TDLDA, for all pairs of sodium clusters, for temperatures ranging from 100 to 500 K and including the temperature-dependent broadening mechanisms mentioned above by folding the electronic response with Gaussian functions with widths in accord with the results of Ref. 37. In keeping with these results, we used the damping ratio $\Gamma/\hbar\omega = 1.2\sqrt{T/C}$, appropriate for the surface fluctuation damping mechanism referred before. For the restoring force coefficient C we used the general scaling expression $C = KN\varepsilon_F$ (cf. Ref. 37) with the constant K fixed by a best fit of this expression with the restoring force coefficients calculated for Na_8 ($\approx$ 16 eV) and Na_{20}($\approx$ 40 eV) making use of the Clemenger–Nilsson model (cf. Ref. 35 and references therein). Furthermore, the width corresponding to the second mechanism mentioned above was taken to be $\Gamma = \gamma T$, with $\gamma = 2$.[36] The largest variation found is always less than 0.1%, which provides additional confidence in the results of Tables 1–6.

Finally, we would like to comment on the accuracy of our estimates. The comparison between the TDLDA results for the dipole polarizability and the experimentally determined photoabsorption cross sections[31] indicate that the TDLDA results are $\approx$ 7% blueshifted with respect to the experimental ones. The FULL-SIC-TDLDA results for neutral sodium clusters with 8 and 20 atoms essentially remove the remaining discrepancies. However, a jellium cluster is certainly a simplification. Irrespective of the remarkable success of this model, it is clear that the jellium model is unable, by itself (and irrespective of the level of sophistication used

in the calculation of the dynamic polarizabilities) to explain very fine details of the photoresponse of clusters to light.[20] While it seems fair to say that the jellium model "works surprisingly well" leading to cross sections which show, sometimes, excellent agreement with the experimental findings, still "jellium" is not the last word, but simply, and likely, an excellent starting point. Therefore, and taking into account the excellent performance of the framework utilized in the present paper in the description of the photoresponse of these microscopic aggregates, we expect that modifications of the values obtained here for C_6 and C_8 will be small.

4. Conclusions and Future Prospects

In this paper, we carried out a state of the art calculation of the nonretarded van der Waals interaction coefficients between pairs of sodium and potassium microclusters. Although lacking experimental data to test the reliability of our results, the success of the model used in reproducing the experimental features of the photo-response of these clusters indicates that our predictions are likely to provide very good estimates for these quantities. From the comparison with the classical calculation, one can conclude that QSE play a crucial role in the determination of these coefficients. A comparison of the results of the two microscopic calculations shows that SIC lead to sizeable changes in the van der Waals coefficients, evidencing how pronounced these effects may be in finite Fermi systems. Relaxation effects are expected to play a minor role, in the sense that they seem unable to change the pattern of Landau fragmentation arising from the microscopic calculation performed in this paper, leading to a marked insensitivity of these coefficients to the vibrational temperature of the clusters.

In the present calculation, the ionic structure and the core electrons have been neglected and replaced by a uniformly charged positive background. It is not clear, at present, the quality of this approximation. Although seemingly very good when applied to neutral sodium clusters,[20] there is indirect information coming from the measurements of the photoresponse of cationic clusters, in which the SJUBM and FULL-SIC-TDLDA are unable to explain the experimental data.[20] Furthermore, it is well known that the core electrons cannot be simply disregarded in the treatment of other metals, such as copper, silver, etc. The improvement upon the approximations used and the application of the present framework to characterize the van der Waals interaction between small particles of other species remains a subject for future work.

References

1. Jacob N. Israelachvili, "Intermolecular and Surface Forces" (Academic Press, 1985).
2. D. Langbein, "Theory of Van der Waals Attraction", *Springer Tracts in Modern Physics* **72** (1974).
3. J. Harris and P. J. Feibelman, *Surf. Sci. Lett.* **115**, L133 (1982).
4. A. N. Castelman *et al.*, *J. Chem. Soc. Faraday Trans.* **86**, 2417 (1990).

5. H. Göhlich *et al.*, *Phys. Rev. Lett.* **65**, 748 (1990); T. P. Martin *et al.*, *J. of Phys. Chem.* **95**, 6421 (1991).
6. W. Krätschmer *et al.*, *Nature* **347**, 354 (1990).
7. S. Wei *et al.*, *Science* **256** 818 (1992).
8. K. Okuyama *et al.*, *J. of Colloid and Interface Sci.* **101**, 98 (1984).
9. A. S. Amadon and W. H. Marlow, *Phys. Rev.* **A43** 5433 (1991) (and references therein).
10. G. Seifert, R. Schmidt, and H. O. Lutz, *Phys. Lett.* **A158** 237 (1991) and references therein.
11. A. Vitturi and C. H. Dasso, "Surface Interaction between Atomic Clusters", preprint, 1992.
12. E. Blaisten-Barojas and M. R. Zachariach, *Phys. Rev.* **B45**, 4403 (1992).
13. O. Gunnarsson *et al.*, *Phys. Rev. Lett.* **67**, 3002 (1991).
14. Ph. Lambin, A. A. Lucas, and J.-P. Vigneron, *Phys. Rev.* **B46**, 1794 (1992).
15. Z. Penzar and M. Šunjić, *Solid. State. Commun.* **54**, 149 (1985).
16. W. Ekardt, *Phys. Rev.* **B29**, 1558 (1984).
17. A. Zangwill and P. Soven, *Phys. Rev.* **B21**, 1561 (1980).
18. W. Ekardt, *Phys. Rev. Lett.* **52**, 1925 (1984).
19. J. P. Perdew and A. Zunger, *Phys. Rev.* **B23**, 5048 (1981).
20. J. M. Pacheco and W. Ekardt, *Ann. Phys. (Leipzig)* 1, 254 (1992).
21. J. M. Pacheco and W. Ekardt, *Z. Phys.* **D24**, 65 (1992).
22. W. Ekardt *et al.*, *Phys. Rev.* **B33**, 3702 (1986).
23. J. M. Pacheco and W. Ekardt, *Phys. Rev. Lett.* **68**, 3694 (1992).
24. A. D. MacLachlan, *Proc. Roy. Soc. London* **A271**, 387 (1963).
25. A. Dalgarno, *Adv. Chem. Phys.* **12**, 143 (1967); *Phys. Rev.* **B31**, 6360 (1985); *Phys. Rev.* **B32**, 1961 (1985).
26. U. Röthlisberger and W. Andreoni, *J. Chem. Phys.* **94**, 8129 (1991).
27. O. Gunnarsson and B. I. Lundqvist, *Phys. Rev.* **B13**, 4274 (1976).
28. The SIC corrections lead to an orbital dependent potential, which in turn leads to eigenfunctions which are not orthogonal. This problem is easily overcome by orthonormalizing the wave functions at each cycle of the self-consistent iteration scheme, and was adopted in all calculations reported in this paper.
29. W. Ekardt and Z. Penzar, *Phys. Rev.* **B43**, 1322 (1991).
30. All dynamic polarizabilities were calculated for $0 \leq \hbar\omega \leq 15$ eV, in steps of 0.01 eV, using an infinitesimal delta $\delta^+ = 10$ meV, which ensures that all curves exhaust the relevant sum-rules (cf. Ref. 18).
31. K. Selby *et al.*, *Phys. Rev.* **B43**, 4565 (1991); C. R. Wang *et al.*, *Chem. Phys. Lett.* **166**, 26 (1990); S. Pollack *et al.*, *J. Chem. Phys.* **94**, 2496 (1991).
32. I. Moullet and J. L. Martins, *J. Chem. Phys.* **92**, 527 (1990).
33. J. M. Standard and P. R. Certain, *J. Chem. Phys.* **83**, 3002 (1985).
34. K. T. Tang *et al.*, *J. Chem. Phys.* **64**, 3063 (1976).
35. J. M. Pacheco and R. A. Broglia, *Phys. Rev. Lett.* **62**, 1400 (1989).
36. C. Yannouleas *et al.*, *Phys. Rev.* **B41**, 6088 (1990).
37. J. M. Pacheco *et al.*, *Z. Phys.* **D21**, 289 (1991).
38. N. Dam and W. S. Saunders, *Z. Phys.* **D19**, 85 (1991).
39. M. Brack *et al.*, *Z. Phys.* **D19**, 51 (1991).